

Salt and Solvent Effects on the Kinetics of the Oxidation of the Excited State of the [Ru(bpy)₃]²⁺ Complex by S₂O₈²⁻

T. Lopes-Costa, P. Lopez-Cornejo, I. Villa, P. Perez-Tejeda, R. Prado-Gotor, and F. Sanchez*

Contribution from: Departamento de Química Física, Facultad de Química, Universidad de Sevilla, c/ Profesor García González s/n, 41012 Sevilla, Spain

Received: September 14, 2005; In Final Form: November 17, 2005

The title reaction was studied in different reaction media: aqueous salt solutions (NaNO₃) and water–cosolvent (methanol) mixtures. The observed rate constants, k_{obs} , show normal behavior in the solutions containing the electrolyte, that is, a negative salt effect. However, the solvent effect is abnormal, because a decrease of the rate constant is observed when the dielectric constant of the reaction medium decreases. These effects (the normal and the abnormal) can be explained using the Marcus–Hush treatment for electron transfer reactions. To apply this treatment, the true, unimolecular, electron-transfer rate constants, k_{et} , have been obtained from k_{obs} after calculation of the rate constants corresponding to the formation of the encounter complex from the separate reactants, k_{D} , and the dissociation of this complex, $k_{-\text{D}}$. This calculation has been carried out using an exponential mean spherical approach (EMSA).

Introduction

Electron-transfer reactions are seen often in chemistry, biology, as well as in industrial fields. They are unique in the sense that, since the pioneering work of Marcus¹ and Hush,² there is a quantitative theoretical framework that allows a deeper insight in the factors controlling the rate of this kind of reaction. Thus, it is well-known that the rate constant for electron-transfer reactions, k_{et} , as given by:³

$$k_{\text{et}} = \kappa_{\text{el}} \nu_n e^{-\Delta G^\ddagger/RT} \quad (1)$$

is controlled by an electronic factor, κ_{el} , a nuclear frequency factor, ν_n , and the activation free energy, ΔG^\ddagger . This free energy can be written as:^{1–3}

$$\Delta G^\ddagger = \frac{(\lambda + \Delta G')^2}{4\lambda} \quad (2)$$

In this equation, λ is the reorganization free energy and $\Delta G'$ is the free-energy change for the electron-transfer step.

For a given electron-transfer reaction, κ_{el} and ν_n are practically fixed so that control on the rate can be achieved through modulation, by the reaction medium, of λ and $\Delta G'$. Consequently, knowledge of how these parameters change when the reaction is carried out in different solvents is important in an understanding of how to control the rate of the reaction. First, it is therefore necessary to obtain k_{et} in different reaction media. It is important to note that for *bimolecular* electron-transfer reactions, like the one studied here, k_{et} is not the datum obtained in a kinetic experiment, k_{obs} . In fact, k_{et} corresponds to the *unimolecular* electron-transfer step, once the donor and the acceptor have formed the precursor complex⁴ (S₂O₈²⁻/Ru(bpy)₃^{2+*} → S₂O₈³⁻/Ru(bpy)₃³⁺, in this case), and k_{obs} corresponds to the process S₂O₈²⁻ + Ru(bpy)₃^{2+*} → S₂O₈³⁻ + Ru(bpy)₃³⁺ (see ref 5).

Under the circumstances prevailing in this work, it can be shown that:

$$k_{\text{obs}} = \frac{k_{\text{D}}k_{\text{et}}}{k_{-\text{D}} + k_{\text{et}}} \quad (3)$$

where k_{D} and $k_{-\text{D}}$ are the rate constants of the forward and backward processes, respectively, in the formation of the precursor complex from the separate reactants.

Consequently, k_{et} can be obtained from k_{obs} after calculations of k_{D} and $k_{-\text{D}}$. Once k_{et} is separated from k_{obs} , ΔG^\ddagger is easily obtained. In this way, λ can be calculated, provided that $\Delta G'^{\circ}$ is known (see eq 2).

Our selection of the reaction studied here was based on the ideas described in the preceding paragraphs: first of all, the free energy for this reaction is very favorable so that eq 3 can be safely applied. Second, as was recently shown by Simonin and Hendrawan,⁶ k_{D} (and $k_{-\text{D}}$) can be calculated to a reasonable accuracy by employing an exponential mean spherical approach (EMSA). Third, redox potentials of the S₂O₈^{2-/3-} couple in the reaction media studied here are available^{7,8} so that by measuring the redox potentials of the [Ru(bpy)₃]^{3+/2+} couple in these media, the reaction free energy can be calculated.

The results presented here can be considered normal in the case of salt solutions: k_{obs} decreases when the concentration of the salt increases. However, the results obtained in the water–methanol mixtures are abnormal according to the conventional theory of solvent effects,⁹ which predicts an increase of the rate constant, k_{obs} , when the dielectric constant of the reaction medium is lowered, whereas here a decrease of k_{obs} is seen. This abnormal effect can be easily rationalized from the data (λ and $\Delta G'$) obtained for the water–methanol mixtures as described previously.

Experimental Section

Materials. Tris (2,2'-bipyridine) ruthenium (III) chloride ([Ru(bpy)₃]Cl₂) from Biomedicals Inc., sodium peroxodisulfate (Na₂S₂O₈) from Fluka, NaNO₃ from Merck, and methanol from

* To whom correspondence should be addressed. E-mail: gcjrv@us.es; Tel. +34-954557175; Fax. +34-954557174.

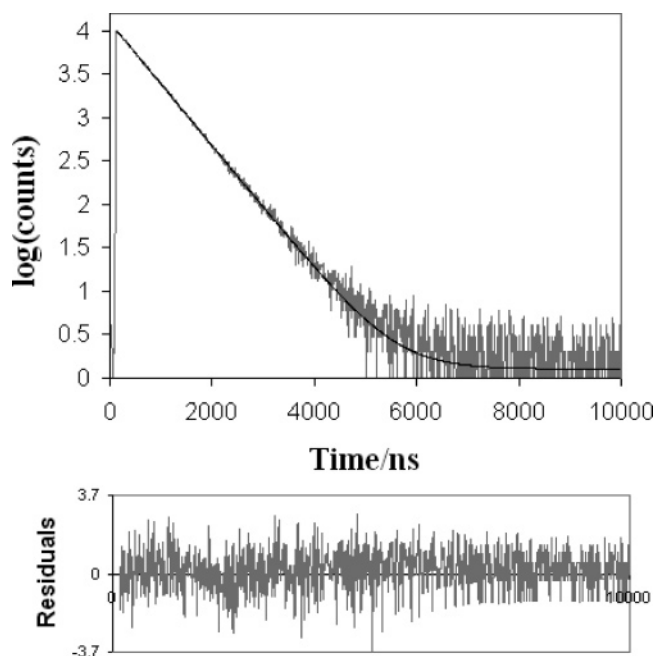


Figure 1. Decay of the excited state of $[\text{Ru}(\text{bpy})_3]^{2+}$ in salt solution ($[\text{NaNO}_3] = 5 \text{ mol dm}^{-3}$) at 298.2 K.

Merck were used as received. All the solutions were prepared with deionized water from a Millipore Milli-Q system, having a conductivity $< 10^{-6} \text{ S m}^{-1}$.

Fluorescence Measurements. (a) Intensity measurements were carried out in a spectrofluorimeter (Hitachi f-2500) interfaced to a PC for the reading and handling of the spectra at 298.2 K. Intensity measurements were performed in the absence of the quencher (I_0) at $[\text{Ru}(\text{bpy})_3]^{2+} = 5 \times 10^{-6} \text{ mol dm}^{-3}$ and in the presence of different quencher ($\text{S}_2\text{O}_8^{2-}$) concentrations ranging from 5×10^{-4} to $3 \times 10^{-3} \text{ mol dm}^{-3}$. In the case of measurements in the presence of the quencher, for water–methanol mixtures, a constant Na^+ concentration was maintained by adding an inert salt (NaNO_3).

(b) Fluorescence lifetimes of the excited state of the ruthenium complex were measured with a FL920 fluorescence lifetime spectrometer from Edinburgh Instruments using the time correlated single-photon counting technique at 298 K. Fluorescence decays were obtained up to 10^4 counts in the peak and were analyzed by an iterative deconvolution procedure based on the Marquardt algorithm.¹⁰ The goodness of the fit was measured by the magnitude χ^2 ($\chi^2 = \sum_i |F_i - f_i|^2$, where F_i is the value of the i th data point and f_i is the value obtained from the fit) and the shape functions of the weighted residuals.

Before lifetime measurements, the solutions were deoxygenated by bubbling argon through them for at least 30 min. Emission and excitation wavelengths were 597 and 452 nm for salt solutions and 594 and 452 nm for cosolvent mixtures. The excitation and emission wavelengths were those that corresponded to the maxima of the absorption and emission spectra, respectively, in the different reaction media.

Figure 1 shows an example of the decay of the excited ruthenium complex and the residuals obtained.

Electrochemistry. Standard formal redox potentials, E° , for the $[\text{Ru}(\text{bpy})_3]^{3+/2+}$ couple:

$$E^\circ = E^\circ + RT \ln \frac{\gamma_{\text{ox}}}{\gamma_{\text{red}}} \quad (4)$$

in the different reaction media were obtained following the

TABLE 1: Stern–Volmer Constants (K_{SV}), Lifetime in the Absence of the Quencher (τ_0), and Observed Rate Constants (k_{obs}) of the Reaction $[\text{Ru}(\text{bpy})_3]^{2+} + \text{S}_2\text{O}_8^{2-}$ in NaNO_3 Salt Solutions at 298.2 K

$[\text{NaNO}_3]$ (mol dm^{-3})	$10^{-2}K_{\text{SV}}$ (mol dm^{-3})	τ_0 (ns)	$10^{-9}k_{\text{obs}}$ ($\text{mol}^{-1}\text{s}^{-1}\text{dm}^3$)
0.009	36.8	603.6	6.10
0.2	7.88	603.4	1.31
0.5	3.87	603.6	0.64
1	1.82	603.5	0.30
2	1.46	603.9	0.24
3	1.27	603.6	0.21
4	1.19	603.7	0.20
5	1.10	603.5	0.18
6	0.97	603.4	0.16

TABLE 2: Stern–Volmer Constants (K_{SV}), Lifetime in the Absence of the Quencher (τ_0), and Observed Rate Constants (k_{obs}) of the Reaction $[\text{Ru}(\text{bpy})_3]^{2+} + \text{S}_2\text{O}_8^{2-}$ in Water–Methanol Mixtures at 298.2 K

% weight (methanol)	$10^{-3}K_{\text{SV}}$ ($\text{mol}^{-1}\text{dm}^3$)	τ_0 (ns)	$10^{-9}k_{\text{obs}}$ ($\text{mol}^{-1}\text{s}^{-1}\text{dm}^3$)
5.68	1.18	531.2	2.22
10.20	1.04	528.8	1.96
18.37	0.85	525.7	1.62
26.53	0.67	522.1	1.28
30.64	0.58	520.6	1.11
39.15	0.40	518.4	0.78

cyclic voltammetry technique as described in ref 11. γ_{ox} and γ_{red} in eq 4 represent the activity coefficients of oxidized and reduced species of the ruthenium complex, respectively. A vitreous carbon working electrode, a saturated calomel reference electrode, and a platinum auxiliary electrode were used in these measurements. A sweep rate of 0.2 V s^{-1} was employed.

In the electrochemical measurements, the concentration of $[\text{Ru}(\text{bpy})_3]^{2+}$ was ranged from 10^{-3} to $1.8 \times 10^{-3} \text{ mol dm}^{-3}$ for salt solutions. In the case of methanol–water mixtures, a concentration of the ruthenium complex equal to $10^{-3} \text{ mol dm}^{-3}$ was used. For the mixtures, NaNO_3 at concentration 0.1 mol dm^{-3} was added.

All the measurements were carried out at 298.2 K.

Results

Table 1 contains the Stern–Volmer constants, K_{SV} , for the salt solutions obtained from:¹²

$$\frac{I_0}{I} = 1 + K_{\text{SV}}[\text{S}_2\text{O}_8^{2-}] \quad (5)$$

The table also contains the lifetimes, τ_0 , in the absence of the quencher, obtained as previously described. From K_{SV} and τ_0 , the observed rate constants, k_{obs} , were obtained ($k_{\text{obs}} = K_{\text{SV}}/\tau_0$).

Table 2 contains the same data as Table 1 but refers to water–methanol mixtures.

In the Stern–Volmer representations, good linear plots were obtained in all cases. As an example, Figure 2 gives the plot corresponding to a water–methanol mixture with a % of weight of methanol of 18.36.

The standard formal redox potentials for the $[\text{Ru}(\text{bpy})_3]^{3+/2+}$ and the $\text{S}_2\text{O}_8^{2-}/\text{S}_2\text{O}_8^{3-}$ (from ref 7) and the $[\text{Ru}(\text{bpy})_3]^{3+/2+}$ couples in salt solutions appear in Table 3. The latter redox potentials were calculated through the equation:¹³

$$E^\circ_{\text{Ru}(\text{bpy})_3^{3+}/\text{Ru}(\text{bpy})_3^{2+}} = E^\circ_{\text{Ru}(\text{bpy})_3^{3+}/\text{Ru}(\text{bpy})_3^{2+}} - E(0-0) \quad (6)$$

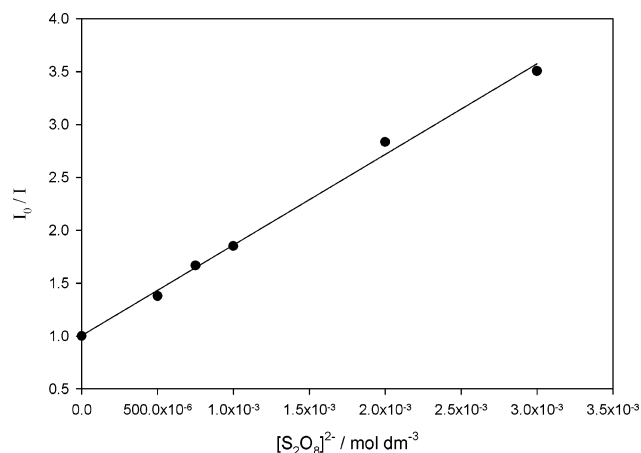


Figure 2. Plot of I_0/I versus the quencher concentration, $[S_2O_8^{2-}]$, in water–methanol mixture (% weight of methanol = 18.37) at 298.2 K.

TABLE 3: Standard Formal Redox Potential (E°/V) Values of the $S_2O_8^{2-}/S_2O_8^{3-}$, $[Ru(bpy)_3]^{3+}/[Ru(bpy)_3]^{2+}$, and the Excited $[Ru(bpy)_3]^{3+}/[Ru(bpy)_3]^{2+*}$ Couples (vs NHE) at Different $NaNO_3$ Concentrations at 298.2 K

[NaNO ₃] (mol dm ⁻³)	$S_2O_8^{2-}/$ $S_2O_8^{3-a}$	$[Ru(bpy)_3]^{3+}/$ $[Ru(bpy)_3]^{2+}$	$[Ru(bpy)_3]^{3+}/$ $[Ru(bpy)_3]^{2+*}$
0.009	1.32	1.34	-0.74
0.2	1.44	1.28	-0.80
0.5	1.48	1.28	-0.81
1	1.50	1.25	-0.83
2	1.53	1.23	-0.85
3	1.55	1.23	-0.85
4	1.56	1.23	-0.86
5	1.57	1.22	-0.86
6	1.57	1.22	-0.86

^a Data taken from ref 7.

TABLE 4: Standard Formal Redox Potential (E°/V) Values of the $S_2O_8^{2-}/S_2O_8^{3-}$, $[Ru(bpy)_3]^{3+}/[Ru(bpy)_3]^{2+}$, and the Excited $[Ru(bpy)_3]^{3+}/[Ru(bpy)_3]^{2+*}$ Couples (vs NHE) in Different Water–Methanol Mixtures at 298.2 K

% weight (methanol)	$S_2O_8^{2-}/$ $S_2O_8^{3-a}$	$[Ru(bpy)_3]^{3+}/$ $[Ru(bpy)_3]^{2+}$	$[Ru(bpy)_3]^{3+}/$ $[Ru(bpy)_3]^{2+*}$
5.68	1.40	1.30	-0.80
10.20	1.40	1.32	-0.78
18.37	1.39	1.35	-0.76
26.53	1.38	1.36	-0.75
30.64	1.38	1.37	-0.74
39.15	1.37	1.39	-0.73

^a Data taken from ref 8.

where $E(0-0)$ corresponds to the 0–0 emission energy. All these potentials are referred to as NHE.

Table 4 contains the standard formal redox potentials in the methanol–water mixtures. Those of the $S_2O_8^{2-}/S_2O_8^{3-}$ couple were from ref 8. As the $S_2O_8^{2-}/S_2O_8^{3-}$ in the table contains the correction of the liquid junction potentials, a similar correction was carried out in the case of $[Ru(bpy)_3]^{3+}/[Ru(bpy)_3]^{2+}$ potentials. To perform this correction, the redox potentials of the $Fe(\mu^5-Cp)_2^+/Fe(\mu^5-Cp)_2^0$ couple (taken from ref 14) were employed.

The redox potentials of the $S_2O_8^{2-}/S_2O_8^{3-}$ couple are close to or higher than those of $[Ru(bpy)_3]^{3+}/[Ru(bpy)_3]^{2+}$; that is, the thermal electron-transfer reaction is allowed from a thermodynamic point of view. However, this reaction is very slow, as we checked in preliminary experiments. Thus, the half-life of this process is ≈ 24 h. As our experiments were carried out in a few seconds, no detectable decrease of the $[Ru(bpy)_3]^{2+}$ is expected during the time of measurements. It is clear from the data in Tables 5 and

6 that the slow rate for the thermal process comes from the high reorganization free energy. This circumstance has also been noted by other authors.²⁵

Calculations

To know the electron-transfer rate constant, k_{et} , that is the rate constant corresponding to process 3b, the value of k_D and k_{-D} (eq 3a) need to be calculated.

The calculations of these diffusion rate constants have been obtained by using the EMSA, following the procedure described in ref 6. In this approach, the ions (reactants and background electrolyte) are characterized by their charges and diameters. k_D is given by:

$$k_D = 4\pi(D_A + D_D)L \quad (7)$$

where D_A and D_D represent the diffusion coefficients of the acceptor ($S_2O_8^{2-}$) and donor ($[Ru(bpy)_3]^{2+*}$), respectively. Parameter L is given by:

$$L^{-1} = \int_{\sigma_r}^{\infty} r^{-2} \exp[\beta V_{AD}^{EMSA}(r)] dr \quad (8)$$

where σ_r is the reaction distance and $V_{AD}^{EMSA}(r)$ is the mean force potential, as given by the EMSA:

$$\beta V_{AD}^{EMSA}(r) = -\frac{G(r)}{r} = \left(\frac{\alpha_{AD}}{r}\right) \frac{1}{(1 + \Gamma r_A)(1 + \Gamma r_D)} \sum_{n=1}^{\infty} G_n(X_n) H(r - r_{\sigma}) \quad (9a)$$

$$\alpha_{AD} = Z_A Z_D \alpha \quad (9b)$$

$$\alpha = \frac{\beta e^2}{4\pi\epsilon_0\epsilon} \quad (9c)$$

In eq 9a, H is the Heaviside and $G(r)$ is defined as:

$$G(r) \equiv r g_{AD}^{el}(r) \quad (10)$$

with g_{AD}^{el} being the electrostatic contribution of the (g_{AD}) radial distribution function. For a more detailed explanation, see refs 6 and 15.

On the other hand, $K_{IP} = k_D/k_{-D}$, which is the equilibrium constant in absence of the quenching reaction, has been calculated from $V_{AD}^{EMSA}(\sigma_r)$, the potential at contact, through:

$$K_{IP} = \exp(-\beta V_{AD}^{EMSA}(\sigma_r)) \quad (11)$$

where σ_r is taken as the contact distance, that is, $\sigma_r = r_A + r_B$.

Once one has K_{IP} and k_D , it is possible to obtain k_{-D} as:

$$k_{-D} = \frac{K_{IP}}{k_D} \quad (12)$$

The values of k_D , k_{-D} , K_{IP} , and k_{et} (this latter from eq 3) are given in Tables 5 and 6 for the salt solutions and the water–methanol mixtures, respectively. The value of K_{IP} corresponding to a solution containing $NaNO_3$ 0.009 mol dm⁻³ is similar to the reported value for the reaction $Ru(NH_3)_5pz^{2+} + S_2O_8^{2-}$ in water by Fürholz and Haim.²⁵ This latter reaction also involves a Ru^{2+} charged complex and $S_2O_8^{2-}$.

A final comment before closing this section. To calculate k_{et} , we have not used the experimental (K_{SV}/τ_0) values of k_{obs} but

TABLE 5: Values of k_D , k_{-D} , K_{IP} , k_{et} , $\Delta G'$, and λ Obtained for Different NaNO₃ Concentrations

[NaNO ₃] (mol dm ⁻³)	10 ⁻⁹ k_D (mol ⁻¹ s ⁻¹ dm ³)	10 ⁻⁹ k_{-D} (s ⁻¹)	K_{IP} (mol ⁻¹ dm ³)	10 ⁻⁷ k_{et} (s ⁻¹)	$\Delta G'$ (kJ mol ⁻¹)	λ (kJ mol ⁻¹)
0.009	16.2	0.73	22	44	-218	418
0.2	10.7	1.31	8.2	18	-225	439
0.5	9.65	1.56	6.2	11	-228	450
1	8.87	1.69	5.2	7.6	-233	465
2	7.79	1.69	4.6	5.5	-235	469
3	6.80	1.57	4.3	4.7	-237	472
4	5.89	1.41	4.2	4.3	-238	474
5	5.05	1.24	4.1	4.1	-238	475
6	4.25	1.07	4.0	4.0	-238	476

TABLE 6: Values of k_D , k_{-D} , K_{IP} , k_{Et} , $\Delta G'$, and λ Obtained for Different Water–Methanol Mixtures.

% weight (methanol)	10 ⁻⁹ k_D (mol ⁻¹ s ⁻¹ dm ³)	10 ⁻⁸ k_{-D} (s ⁻¹)	K_{IP} (mol ⁻¹ dm ³)	10 ⁻⁷ k_{et} (s ⁻¹)	$\Delta G'$ (kJ mol ⁻¹)	λ (kJ mol ⁻¹)
5.68	12.2	5.09	24	11	-222	440
10.20	11.4	4.52	25	9.5	-220	441
18.37	9.47	3.39	28	6.7	-218	442
26.53	8.66	2.75	32	4.6	-216	445
30.64	8.48	2.52	34	3.8	-215	447
39.15	8.51	2.19	39	2.5	-214	451

the values of this rate constant resulting from the fit of these experimental values to (see Figures 3 and 4):¹⁶

$$k_{\text{obs}} = \frac{k_0 + Kk_1[\text{NaNO}_3]}{1 + K[\text{NaNO}_3]} \quad (13)$$

for salt solutions, and to eq 14 for water–methanol mixtures:¹⁷

$$k_{\text{obs}} = \frac{k_0 + Kk_1x}{1 + Kx} \quad (14)$$

where x represents the ratio between the mole fractions of the methanol and water.

Discussion

(a) Salt Effects. According to the data in Table 1, the expected negative salt effect was observed for the reaction studied here, taking into account that the reactants are ions of opposite charge. Moreover, according to data in Table 5, k_{et} decreases with the salt concentration. That is, a negative salt effect on k_{et} is observed so that the negative (global) salt effect arises from the effect of the salt on the diffusion step (k_D) and on the electron-transfer step.

To take a deeper insight into the negative salt effect on k_{et} , the Marcus–Hush formulation for electron-transfer reactions, as given in eq 1, was used. In this equation, the pre-exponential term, $\kappa_{el} \nu_n$, can be considered independent of the reaction medium. This term, except for strongly nonadiabatic processes, is of the order of the (average) vibratory frequency promoting the activation of the precursor complex. Thus, a value of 10¹²–10¹³ s⁻¹ seems reasonable. In the calculations, we used a value of 6.62 × 10¹² s⁻¹. This value corresponds to the value of the pre-exponential factor in the expression of the rate constant given by the classical transition state theory ($k_B T/h$) at the working temperature. In this way, ΔG^\ddagger can be obtained from k_{et} (see eq 1).

Once ΔG^\ddagger has been calculated, it is possible to obtain the two parameters, λ and $\Delta G'$, which, according to eq 2, appear in ΔG^\ddagger . It is important to realize that $\Delta G'$ is not the standard formal reaction free energy, $\Delta G^{\circ'}$, of the reaction:

$$\Delta G^{\circ'} = -nF(E^{\circ'}_{\text{S}_2\text{O}_8^{2-/\text{S}_2\text{O}_8^{3-}} - E^{\circ'}_{\text{Ru}(\text{bpy})_3^{3+/2+}}) \quad (15)$$

However, $\Delta G'$ and $\Delta G^{\circ'}$ are related through:

$$\Delta G' = \Delta G^{\circ'} + w_p - w_r \quad (16)$$

Here, w_r and w_p are the free energies corresponding to the formation of the precursor complex from the separate reactants and the formation of the successor complex from the separate products.

w_r was calculated as:

$$w_r = -RT \ln K_{IP} \quad (17)$$

from the values of K_{IP} appearing in Table 5. As for the w_p values, $w_p = (9/4)w_r$ was used, taking into account that the product of the charges of the ions forming the successor complex (S₂O₈³⁻ and [Ru(bpy)₃]³⁺) is 9/4 of the product of the charges of the reactants. In this way, the values of $\Delta G'$ and λ given in Table 5 were obtained.

It is clear that the negative salt effect on k_{et} arises from the fact that although the electron-transfer step becomes more favorable from a thermodynamic point of view when the concentration of the salt increases, this is not enough to compensate for the increase of λ . The fact that the reaction becomes more favorable thermodynamically speaking is a consequence of S₂O₈²⁻ being a more powerful oxidant in the presence of the salt and [Ru(bpy)₃]²⁺* a more reductant species. This is clearly seen in eq 4, which gives the standard formal redox potential of a given couple. For the S₂O₈²⁻/S₂O₈³⁻ couple, both γ_{ox} and γ_{red} decrease with increasing salt concentration. However, the decrease in γ_{red} is more marked because of the higher (absolute) charge of the reduced form of this couple. Thus, $E^{\circ'}$ increases as the salt concentration does. The opposite is true for the cationic, Ru(bpy)₃³⁺/Ru(bpy)₃²⁺* couple. Consequently, the reaction becomes more favorable thermodynamically. Notice that parameter λ causes the negative salt effect on k_{et} , as this parameter increases as the concentration of the salt is increased, in agreement with the theoretical treatment of the salts effects on this reorganization free energy.¹⁸

(b) Solvent Effects. In many ways, the results obtained for the water–methanol mixtures are the most interesting results of this work. They correspond to an unexpected solvent effect, as k_{obs} decreases when the content of methanol increases. To a small extent, this is due to a decrease in the rate of the diffusion step (k_D). However, the main cause is the diminution of the k_{et} .

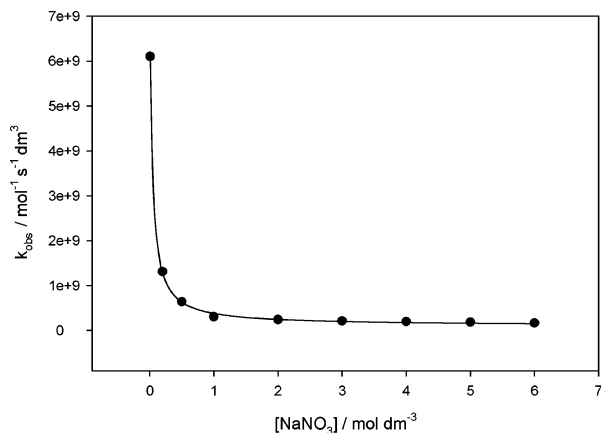


Figure 3. Plot of the rate constant k_{obs} versus the NaNO_3 concentration at 298.2 K.

This diminution can be considered in detail using the same approach as in the case of salt effects. Thus, we calculated the values of $\Delta G'$ and λ in the water–methanol mixtures. They appear in Table 6.

It can be clearly seen from this table that both the variation of the free energy of the electron-transfer step and the reorganization energy of this step produce a diminution of k_{et} , because both of them increase when the reaction medium becomes richer in methanol content.

The increase of $\Delta G'$ can again be explained using eq 4: when the dielectric constant of the reaction medium decreases, both γ_{ox} and γ_{red} will increase. For the $\text{S}_2\text{O}_8^{2-}/\text{S}_2\text{O}_8^{3-}$ couple, γ_{ox} will increase less than γ_{red} because the oxidized form of this couple bears a lower (absolute) charge. In this way, the $\text{S}_2\text{O}_8^{2-}$ becomes a less powerful oxidant when the methanol content is increased. The ruthenium complex becomes less reductant in this case. Thus, a less favorable $\Delta G'$ is seen when the amount of the alcohol in the reaction medium increases.

The increase of λ in water–methanol mixtures is somewhat unexpected. This reorganization free energy contains an internal contribution, λ_{in} , arising from the internal reorganization of the bonds of the donor and the acceptor, and a solvent contribution, λ_{s} , arising from the solvent reorganization. The internal contribution can be considered as independent of the reaction medium. However, λ_{s} depends on the solvent:^{1,2}

$$\lambda_{\text{s}} = N_{\text{A}} e^2 \left(\frac{1}{2r_{\text{A}}} + \frac{1}{2r_{\text{D}}} - \frac{1}{dr} \right) \gamma = A\gamma \quad (18)$$

As the Pekar's factor, γ , given by:

$$\gamma = \frac{1}{n^2} - \frac{1}{\epsilon} \quad (19)$$

decreases when the content of methanol increases, λ_{s} and, thus, λ should decrease. However, the opposite trend is observed in Table 6.

To explain the increase of λ , it is important to realize that our data correspond to solvent mixtures instead of neat solvents. In these mixtures, when the electron transfer happens, both reactants change their charges, and consequently, a modification of the composition of their solvations shells is expected (this modification, of course, is absent in neat solvents). This change in the composition of the solvation shells will produce an extra reorganization of the solvent, caused by a translational movement of some solvent molecules, because in the transition state, the position of the molecules of the two components of the

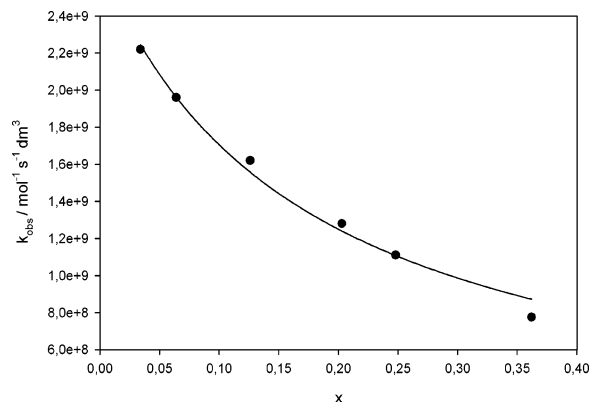


Figure 4. Plot of the rate constant k_{obs} versus the relative molar fraction x (see text in Calculations Section) at 298.2 K.

solvent (and not only the solvent polarization) will be intermediate between the positions corresponding to the (preferential) solvation of the precursor and successor complexes. The cause of the extra component in λ is not the preferential solvation itself but the changes in this preferential solvation in the activation process, which implies a movement of solvent molecules in the activation step.

This component of the reorganization energy has been observed by some of the present authors in previous works¹⁹ as well as by other authors. Thus, Curtis et al.²⁰ suggested this extra contribution from the results obtained through thermodynamic (redox) measurements corresponding to some inorganic complexes in solvent mixtures. A similar conclusion was reached by Hupp et al.²¹ from the study of the spectra of some complexes in solvent mixtures. Moreover, the existence of this extra component of the solvent reorganization energy in solvent mixtures has been predicted theoretically by Matyushov²² and corroborated through simulations.²³

According to the previous interpretation, in solvent mixtures, a component of the reorganization energy, not included in eq 20, must exist to produce an increase in λ when the amount of the alcohol increases and, thus, the Pekar's factor decreases. This component can be estimated as follows; assigning λ_{ex} as this extra component of the reorganization free energy, it can thus be written for the water–methanol mixtures:

$$\lambda_{\text{ex}} = \lambda - \lambda_{\text{in}} - \lambda_{\text{s}} \quad (20)$$

Thus, according to previous arguments, this component does not exist in pure solvents, in water for example, and it can be written:

$$\lambda_{\text{in}} = \lambda_{\text{H}_2\text{O}} - (\lambda_{\text{s}})_{\text{H}_2\text{O}} \quad (21)$$

In principle, λ_{s} for water would be calculated from eq 18. However, this equation has been questioned because it overestimates λ_{s} .²⁴ For this reason, we preferred to estimate λ_{in} using published data. Thus, λ_{in} for $\text{S}_2\text{O}_8^{2-}$ was established to be about 660 kJ mol⁻¹.²⁵ For the ruthenium complex, a value of λ_{in} of 2 kJ mol⁻¹ was used.²⁶ Consequently, a value of 331 kJ mol⁻¹ is obtained. Using this value, λ_{s} for water is calculated as 87.7 kJ mol⁻¹. Thus, the effective value of parameter A in eq 18 is:

$$A = \frac{(\lambda_{\text{s}})_{\text{H}_2\text{O}}}{\gamma_{\text{H}_2\text{O}}} = 159.4 \text{ kJ mol}^{-1} \quad (22)$$

Using this value of A to calculate λ_{s} in eq 20, as well as the value of λ_{in} previously estimated, the values of λ_{ex} appearing in Table 7 are obtained.

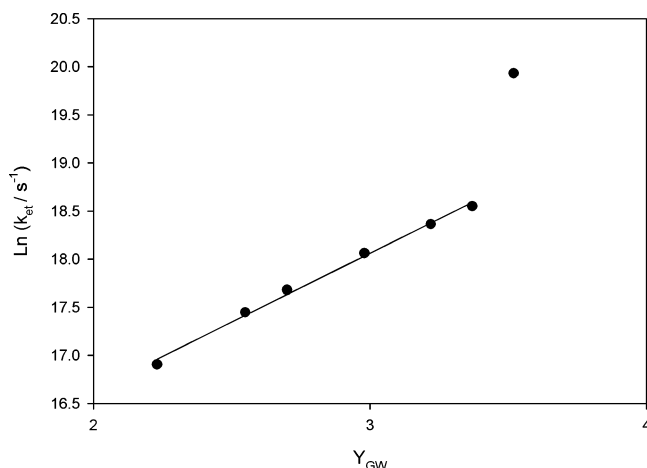


Figure 5. Plot of $\ln k_{\text{et}}$ versus the Grunwald–Winstein polarity parameter, Y_{GW} , in water–methanol mixtures.

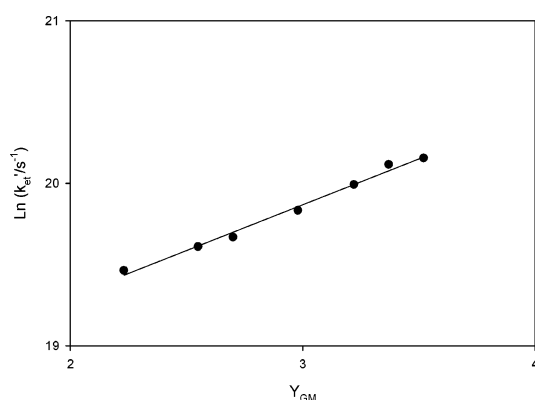


Figure 6. Plot of $\ln k'_{\text{et}}$ versus the Grunwald–Winstein polarity parameter, Y_{GM} , in water–methanol mixtures.

TABLE 7: Values of λ_{ex} and k'_{et} Obtained for Different Water–Methanol Mixtures

% weight (methanol)	λ_{ex} (kJ mol ⁻¹)	$10^{-8}k'_{\text{et}}$ (s ⁻¹)
5.68	22	5.5
10.20	23	4.8
18.37	25	4.1
26.53	27	3.5
30.64	29	3.3
39.15	34	2.8

To have an idea of the accuracy of this estimation of λ_{ex} , consider Figure 5. In this figure, $\ln k_{\text{et}}$ has been plotted versus the Grunwald–Winstein polarity parameter, Y_{GW} , corresponding to the water–methanol mixtures.²⁷ A good linear plot is obtained if the water point is excluded.

This behavior could be due to two reasons: the values of k_{et} corresponding to the mixtures are too low, or the value of k_{et} corresponding to the water must be lower than the value obtained experimentally. Next, we can calculate the electron-transfer constant of this process without the extra component of the reorganization free energy for the water–methanol mixtures. This electron-transfer constant, k'_{et} , can be calculated using the eq 23:

$$k'_{\text{et}} = \frac{k_{\text{B}}T}{h} \exp\left(\frac{(\lambda - \lambda_{\text{ex}} + \Delta G')^2}{4(\lambda - \lambda_{\text{ex}})RT}\right) \quad (23)$$

The values of k'_{et} are given in Table 7, and plotted versus Y_{GM} in Figure 6. It can be seen in this figure that the water

point is now included in the general plot. This supports our estimation of λ_{ex} .

Conclusions

In this work we have studied the oxidation of $[\text{Ru}(\text{bpy})_3]^{2+}$ by $\text{S}_2\text{O}_8^{2-}$ in salt solutions and in water–methanol mixtures. Using an extended mean spherical approach (EMSA) and the Marcus–Hush formulation for electron-transfer reactions, it was possible to explain the normal salt effects and the abnormal solvent effects. The latter is a consequence of the fact that: (i) in water–methanol mixtures, the reaction becomes less favorable thermodynamically speaking and (ii) in these mixtures, an extra contribution of the solvent reorganization free energy appears.

Acknowledgment. This work was financed by the D.G.I.-C.Y.T. (BQU 2002-01063) and the Consejería de Educación y Ciencia de la Junta de Andalucía. Two of the authors thank Ministerio de Ciencia y Tecnología (MCYT) and Ministerio de Educación y Ciencia (MEC) for their financial support through Grants BES-2003-1219 and AP 2003-1155.

References and Notes

- (1) Marcus, R. A. *Annu. Rev. Phys. Chem.* **1964**, *15*, 155, and references therein.
- (2) Hush, N. S. *J. Chem. Phys.* **1958**, *28*, 962.
- (3) Marcus, R. A.; Sutin, N. *Biochim. Biophys. Acta* **1985**, *811*, 265.
- (4) Sanchez Burgos, F.; Moyá, M. L.; Galán, M. *Prog. React. Kinet.* **1994**, *19*, 1.
- (5) After this rate-determining step, $\text{S}_2\text{O}_8^{3-}$ decomposes and produces $\text{SO}_4^{2-} + \text{SO}_4^{\bullet-}$. The $\text{SO}_4^{\bullet-}$ radical anion oxidizes a second ruthenium complex in a rapid (non-rate-determining) step.
- (6) Simonin, J. P.; Hendrawan, H. *PCCP*, **2001**, *3*, 4286.
- (7) Rodriguez, A.; López-Cornejo, P.; Muriel, F.; Sánchez, F.; Burgess, J. *Int. J. Chem. Kinet.* **1999**, *31*, 485.
- (8) Sánchez, F.; Rodriguez, A.; Muriel, F.; Burgess, J.; López-Cornejo, P. *Chem. Phys.* **1999**, *243*, 159.
- (9) Laidler, K. J. *Chemical Kinetics*, 2nd ed.; McGraw-Hill: London, 1965; pp 202 ff.
- (10) Marquardt, D. W. *J. Soc. Pure Appl. Math.* **1963**, *11*, 431.
- (11) Roldan, E.; Dominguez, M.; Gonzalez-Arjona, D. *Comput. Chem.* **1986**, *10*, 187.
- (12) Rodríguez, A.; de la Rosa, F.; Galán, M.; Sánchez, F.; Moyá, M. L. *Photochem. Photobiol.* **1992**, *55*, 367.
- (13) Berg-Brennan, C.; Subramanian, P.; Absi, M.; Stern, C.; Hupp, J. T. *Inorg. Chem.* **1996**, *35*, 3719.
- (14) Matamoros-Fontela, M. S.; Perez, P.; López, P.; Prado-Gotor, R.; De la Vega, R.; Sánchez, F. *Ber. Bunsen-Ges. Phys. Chem.* **1997**, *101*, 1452.
- (15) Blum, L.; Hoyer, J. S. *J. Phys. Chem.* **1977**, *81*, 1311.
- (16) Olson, A. R.; Simonson, T. R. *J. Chem. Phys.* **1949**, *17*, 1167.
- (17) Perez-Tejeda, P.; Franco, F. J.; Sánchez, A.; Morillo, M.; Denk, C.; Sánchez, F. *PCCP* **2001**, *3*, 1271.
- (18) Pérez-Tejeda, P.; Jiménez Sindreu, R.; López-Cornejo, P.; Sánchez Burgos, F. *Curr. Top. Solution Chem.* **1997**, *2*, 49.
- (19) Morillo, M.; Denk, C.; Perez, P.; Lopez, M.; Sánchez, A.; Prado, R.; Sánchez, F. *Coord. Chem. Rev.* **2000**, *204*, 173 and references therein.
- (20) Curtis, J. C.; Blackburn, R. L.; Ennix, K. S.; Roberts, J. A.; Hupp, J. T. *Inorg. Chem.* **1989**, *28*, 3791.
- (21) (a) Hupp, J. T. *Inorg. Chem.* **1987**, *26*, 2657. (b) Blackburn, R. L.; Doorn, S. K.; Roberts, J. A.; Hupp, J. T. *Langmuir* **1989**, *5*, 696.
- (22) (a) Matyushov, D. V. *Mol. Phys.* **1993**, *79*, 795. (b) Karasevskii, A. I.; Matyushov, D. V.; Gorodyskii, A. V. *Chem. Phys.* **1990**, *142*, 1.
- (23) Denk, C.; Morillo, M.; Sánchez-Burgos, F.; Sánchez, A. *J. Chem. Phys.* **1999**, *110*, 473.
- (24) Karki, L.; Lu, M. P.; Hupp, J. T. *J. Phys. Chem.* **1996**, *100*, 15637.
- (25) Fürholz, U.; Haim, A. *Inorg. Chem.* **1987**, *26*, 3243.
- (26) In fact, the value corresponds to the $\text{Fe}(\text{bpy})_3^{2+}$. However, as this value is small, its contribution to the total value of λ_{in} is not significant (Terretaz, S.; Becka, A. M.; Traub, M. J.; Felting, J. C.; Miller, C. J. *J. Phys. Chem.* **1995**, *99*, 11216).
- (27) Moyá, M. L.; Sánchez, F.; Burgess, J. *Int. J. Chem. Kinet.* **1993**, *25*, 891 and references therein.